Molecular View on Mechanical Reinforcement in Polymer Nanocomposites

Ruikun Sun,[1] Matthew Melton,[1] Niloofar Safaie,[2] Robert C. Ferrier, Jr.,[1]
Shiwang Cheng,[1,*] Yun Liu,[3,4] Xiaobing Zuo,[5] and Yangyang Wang[6,†]

[1]*Department of Chemical Engineering and Materials Science, Michigan State University, East Lansing, Michigan 48824, USA*
[2]*Department of Chemistry, Michigan State University, East Lansing, Michigan 48824, USA*
[3]*Center for Neutron Research, National Institute of Standards and Technology, Gaithersburg, Maryland 20899, USA*
[4]*Department of Chemical and Biomolecular Engineering, University of Delaware, Newark, Delaware 19716, USA*
[5]*X-ray Science Division, Argonne National Laboratory, Lemont, Illinois 60439, USA*
[6]*Center for Nanophase Materials Sciences, Oak Ridge National Laboratory, Oak Ridge, Tennessee 37831, USA*

(Dated: August 12, 2021)

The microscopic origin of mechanical enhancement in polymer nanocomposite (PNC) melts is investigated through the combination of rheology and small-angle neutron scattering. It is shown that in the absence of an extensive particle network, the molecular deformation of polymer chains dominates the stress response on intermediate time scales. Quantitative analyses of small-angle neutron scattering spectra, however, reveal no enhanced structural anisotropy in the PNCs, compared with the pristine polymers under the same deformation conditions. These results demonstrate that the mechanical reinforcement of PNCs is not due to the molecular overstraining, but instead a redistribution of strain field in the polymer matrix, akin to the classical picture of hydrodynamic effect of nanoparticles.

Incorporation of nanoparticles (NPs) into a polymer matrix can significantly improve the mechanical performance of the resulting polymer nanocomposites (PNCs) [1–4]. Despite the wide recognition of the reinforcement effect of NPs, the molecular origin of this phenomenon remains largely elusive [5–8]. Inspired by Einstein's insights on the hydrodynamic effect [9, 10], Smallwood demonstrated that the modulus of the filled rubber is enhanced in a similar manner as the viscosity of dilute suspensions of particles, where the particle alters the strain distribution of its surrounding medium [11, 12]. While the Einstein-Smallwood relation describes well the mechanical enhancement of PNCs at dilute conditions, the theory of hydrodynamic reinforcement at high concentrations has not been fully established [13], particularly in the nonlinear rheological regime. Moreover, despite the critical insight offered by the hydrodynamic theory on the mechanical reinforcement of PNCs, the fundamental question of how the NPs affect the deformation of the matrix polymer and why the presence of NPs can lead to the high mechanical strength of PNCs are still under active debate. For instance, Mullins attributed the high mechanical stiffness of filled rubbers to larger effective deformation of the matrix polymer relative to the unfilled state, invoking the concept of strain amplification or molecular overstraining [14]. Although the concept of strain amplification is widely employed by the PNCs community [7, 15–18], microscopic experiments regarding its existence have been inconclusive and controversial. On the one hand, an early small-angle neutron scattering (SANS) [16] and a more recent H-NMR spectroscopy measurements [17] showed signs of strain amplification in rubber composites; on the other hand, recent SANS experiments [19, 20] claimed no evidence of molecular overstraining in rubber/silica and polystyrene/silica nanocomposites, and nanoparticle-nanoparticle interaction was offered as the explanation for mechanical reinforcement in the melt state. Because of these seemingly conflicting results, our current understanding about the microscopic consequence of hydrodynamic reinforcement has been murky and incomplete.

Motivated by this challenge, we set out to examine the length scale dependent structural anisotropy of deformed polymer nanocomposites and reveal the molecular origin of mechanical reinforcement through a combination of small-angle neutron scattering and rheology. Unlike the previous SANS studies on this subject [16, 20–23], the current work applies spherical harmonic expansion (SHE) analysis [24–26] to accurately quantify the anisotropic structure of the polymer matrix across a wide range of length scales. Additionally, the combination of SANS and rheology allows a clear evaluation of the stress contributions from different components, in contrast to the previous investigations, where only a single technique was employed. Most importantly, our results show unambiguously a lack of molecular overstraining of the polymer matrix at all length scales, ruling out the strain amplification of the bulk polymer as the mechanism for the mechanical reinforcement of PNCs.

Poly(methyl methacrylate) (PMMA) with 8 vol% 8-nm-radius silica nanoparticles serves as a model system in this study. To probe the molecular deformation of the polymer matrix with small-angle neutron scattering, deuterated (D^8-PMMA, $M_w = 217$ kg/mol, PDI = 1.27) and hydrogenous PMMAs (H^8-PMMA, $M_w = 194$ kg/mol, PDI = 1.08) are mixed at an H/D ratio of 0.59:0.41 to match the scattering length density of the SiO_2 nanoparticles. The the leveling off of the scattering intensity at low Q ($Q < 0.006$ Å^{-1}) of the small-angle x-ray scattering spectrum (12-ID-B beamline, APS) and TEM

* chengsh9@msu.edu
† wangy@ornl.gov

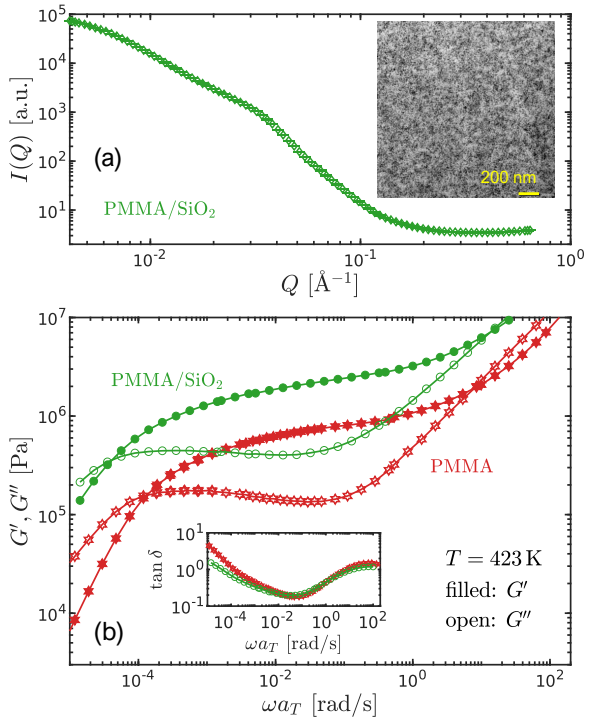

FIG. 1. (a) Small-angle x-ray scattering spectrum of PMMA/SiO_2. Inset: TEM image of the same sample. (b) Linear viscoelastic spectra of PMMA and PMMA/SiO_2 at 423 K . These mastercurves are constructed using the time-temperature superposition principle [27]. Here, ω is the angular frequency and a_T is the shift factor. Stars: PMMA. Circles: PMMA/SiO_2. Inset: loss factor $\tan\delta(\omega) \equiv G''(\omega)/G'(\omega)$.

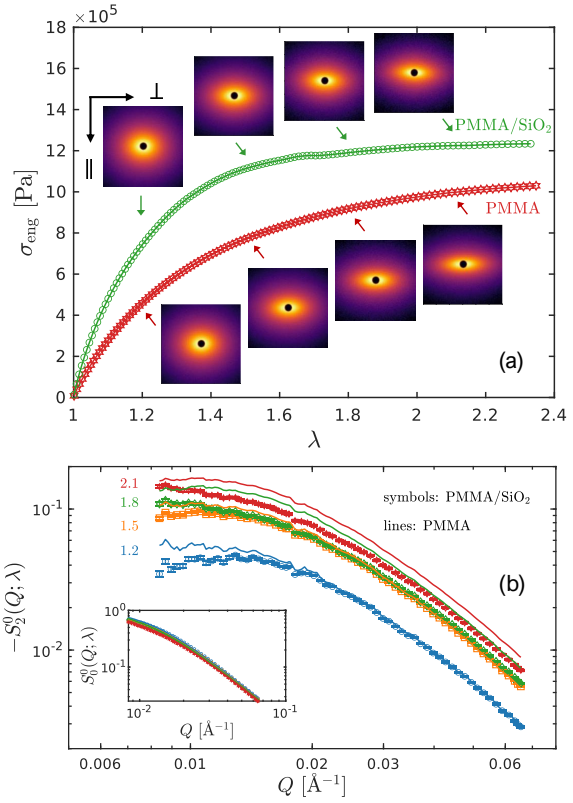

FIG. 2. (a) Stress-strain curves of PMMA and PMMA/SiO_2 at a constant Hencky strain rate of $\dot{\varepsilon} = 0.01\ \mathrm{s}^{-1}$ at $T = 423$ K, along with the SANS spectra taken at stretching ratios of 1.2, 1.5, 1.8, and 2.1. We point out that the stress enhancement at large strains, ca. 23%, is consistent with the hydrodynamic effect of nanoparticles from the Padé approximation. (b) Spherical harmonic expansion coefficients. Here, $S_0^0(Q)$ and $S_2^0(Q)$ are respectively the isotropic and leading anisotropic expansion coefficients of the structure factor $S(\mathbf{Q})$. Symbols: PMMA/SiO_2. Lines: PMMA.

image in Fig. 1a indicate an absence of an extensive nanoparticle network in the PNC. This conclusion is further supported by the linear viscoelastic spectra of the pristine PMMA and PMMA/SiO_2 in Fig. 1b, where the two samples exhibit almost identical loss factors, $\tan\delta \equiv G''/G'$, in the entire rubbery plateau region (Fig. 1b inset). On the other hand, the presence of NPs in PMMA/SiO_2 leads to a threefold increase of plateau modulus, compared to the pristine PMMA. These rheological and structural properties clearly show that the mechanical reinforcement in PMMA/SiO_2 is dominated by the hydrodynamic effect, rather than a network due to percolation of nanoparticles. This makes PMMA/SiO_2 an ideal candidate for SANS investigations of the influence of NPs on the molecular deformation of the matrix polymer. The details of the sample preparation, characterization, and methods are presented in the Supplemental Material (SM) [12].

We apply the zero average contrast (ZAC) method [28] to characterize the molecular deformation of the polymer matrix on different length scales by SANS, which is a key for clarifying the microscopic consequences of hydrodynamic reinforcement. The details of identification of the ZAC point are described in the SM. We first focus on the analysis of evolution of structural anisotropy during continuous uniaxial extension. The pristine PMMA and PMMA/SiO_2 were stretched with a constant Hencky strain rate of $\dot{\varepsilon} = 0.01\ \mathrm{s}^{-1}$ at $T = 423$ K to different elongation ratios, followed by a fast quench to room temperature to preserve the molecular deformation (see SM [12]). The SANS spectra of these glassy samples were then measured at the NGB 30m SANS beamline at NCNR.

Figure 2a presents the stress-strain curves of PMMA and PMMA/SiO_2, along with the 2D SANS spectra at $\lambda = 1.2, 1.5, 1.8$, and 2.1. While the presence of NPs significantly enhances the mechanical stress (green circles), there is no appreciable difference between the SANS spectra of the two samples. We employ the spherical harmonic expansion analysis to further quantify the structural anisotropy from the 2D SANS spectra (see Ref. [26] and the SM [12] for details). This technique decomposes the SANS spectra into contributions from different symmetries and allows a clear separation of isotropic and anisotropic spectral components. Under the ideal ZAC condition, the coherent scattering intensity $I_{\mathrm{coh}}(\mathbf{Q})$ of PMMA/SiO_2 should be proportional to the single-chain structure factor $S(\mathbf{Q})$ of PMMA [24, 29]: $I(\mathbf{Q}) \approx I_{\mathrm{coh}}(\mathbf{Q}) = \phi_{\mathrm{pol}}\phi_{\mathrm{H}}\phi_{\mathrm{D}}n_{\mathrm{seg}}(b_{\mathrm{D}} - b_{\mathrm{H}})^2 NS(\mathbf{Q})$, where ϕ_{pol}

is the polymer volume fraction, ϕ_H and ϕ_D are respectively the volume fractions of hydrogenous and deuterated chains, n_{seg} is the polymer number density, b_D and b_H are respectively the coherent scattering length of the deuterated and hydrogenous chain segments, N is the degree of polymerization (number of segments per chain), and $S(\mathbf{Q})$ is the single-chain structure factor. For uniaxial extension, $S(\mathbf{Q})$ can be expressed as a linear combination of even degree spherical harmonic functions $Y_l^0(\theta,\phi)$ with Q-dependent expansion coefficients $S_l^0(Q)$:

$$S(\mathbf{Q}) = \sum_{l:\text{even}} S_l^0(Q) Y_l^0(\theta,\phi), \tag{1}$$

with θ being the polar angle and ϕ the azimuthal angle. A schematic representation of the scattering geometry is included in the SM [12]. Experimentally, the coefficients $S_l^0(Q)$ can be obtained from weighted angular integrals of the SANS spectra:

$$S_l^0(Q) = \frac{1}{2}\int_0^\pi I_{xz}(Q,\theta) Y_l^0(\theta)\sin\theta\, d\theta \Big/ \lim_{Q\to 0} I_{\text{iso}}(Q). \tag{2}$$

Here, $I_{xz}(Q,\theta)$ is the intensity measured on the 2D detector plane (xz plane) and $\lim_{Q\to 0} I_{\text{iso}}(Q)$ is the zero-angle scattering of the isotropic sample. Our previous analysis (Supplemental Material of Ref. [25]) demonstrates that the tensile stress ($\sigma_{zz}-\sigma_{xx}$) of Gaussian chains is determined by the two-point spatial correlations associated with only the spherical harmonic function $Y_2^0(\theta,\phi)$: $\sigma_{zz}-\sigma_{xx} = 2\nu\beta^2 k_B T\left[\frac{1}{\sqrt{5}}\int_0^\infty 4\pi r^2 \psi_2^0(r) r^2\, dr\right]$, where ν is the number density of "load-bearing strands," $\beta^2 \equiv 3/2sb^2$, with s being the number of beads in the strand and b the bead size, and $\psi_2^0(r) = \frac{1}{4\pi}\int \psi(\mathbf{r}) Y_2^0(\theta,\phi)\, d\theta d\phi$ is the leading anisotropic expansion coefficient of the strand configuration distribution function $\psi(\mathbf{r})$. While a direct connection between $S_2^0(Q)$ and stress is yet to be established, in the small-strain limit, it can be shown with the affine deformation model that the molecular strain is approximately proportional to the peak amplitude of the $S_2^0(Q)$ [12]. In other words, the structural anisotropy determined from the ZAC SANS experiments should reflect the contribution of the polymer matrix to the total stress.

Figure 2b shows the spherical harmonic expansion analysis of the PNC (symbols) and the pristine polymer (lines). On the one hand, the leading anisotropic terms $S_2^0(Q;\lambda)$ of both the pristine polymer and the PNC increase with the stretching ratio λ in the Q range of 0.008-0.065 Å^{-1}. On the other hand, the isotropic coefficients $S_0^0(Q;\lambda)$ of the pristine polymer and the PNC (inset of Figure 2b) exhibit no discernible difference across all Qs. This observation underscores the advantage of the spherical harmonic expansion technique over the traditional analysis of scattering intensities in parallel and perpendicular directions, where the contributions from isotropic and anisotropic coefficients are not isolated. More details of the differences between the SHE analysis and traditional analysis are presented in the SM [12]. Note that the previous SANS experiment [16] relied heavily on model assumptions to characterize polymer microscopic deformation, producing large uncertainties especially under imperfect ZAC condition. From

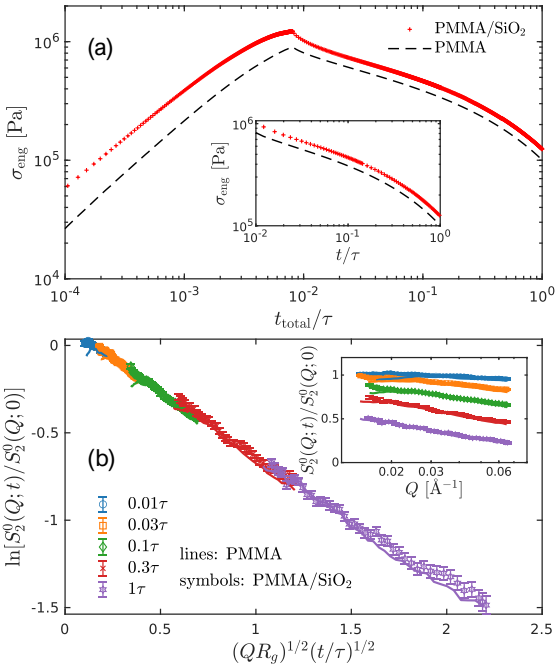

FIG. 3. (a) Evolution of engineering stress σ_{eng} of PMMA (lines) and PMMA/SiO_2 (symbols) during a step uniaxial extension performed with $\dot{\varepsilon} = 0.01$ s^{-1} at $T = 423$ K and the subsequent stress relaxation. The time t is normalized by the terminal relaxation time τ of the pristine PMMA. Inset: engineering stress during relaxation. (b) PMMA and PMMA/SiO_2 exhibit identical scaling behavior for anisotropy relaxation. $S_2^0(Q;0)$ is the expansion coefficient immediately after the step deformation, whereas $S_2^0(Q;t)$ is the coefficient during the stress relaxation. Inset: spatial dependence of the normalized expansion coefficient $S_2^0(Q;t)/S_2^0(Q;0)$ during the relaxation.

the perspective, the separation of isotropic and anisotropic spectral components by the SHE analysis permits a quantitative examination of the molecular overstraining idea. Remarkably, the $S_2^0(Q;\lambda)$ of the PMMA/SiO_2 is almost identical to that of the pristine PMMA across the whole Q range at $\lambda = 1.2$ and 1.5. Moreover, at larger deformation of λ = 1.8 and 2.1, the magnitude of $S_2^0(Q;\lambda)$ of the PNC appears to be slightly smaller than the pristine polymer, implying the presence of NPs reduces the average deformation of the polymer matrix rather than amplifying it. By contrast, the stress in PMMA/SiO_2 is approximately 100% (at $\lambda \to 1.2$) to 23% (at $\lambda = 2.1$) higher than that in the PMMA. In other words, a naïve application of the strain amplification concept should predict significantly higher structural anisotropy, which we clearly do not observe in the SANS experiments.

The lack of increased structural anisotropy from the SANS measurements and the significant mechanical enhancement in both the linear and nonlinear rheological regimes beg an explanation: where does the extra stress come from? It was previously suggested that direct filler-filler interactions are the main cause for such a phenomenon [19, 20]. To critically test this hypothesis, we proceeded to perform stress relaxation experiments. Because of the slow nature of particle Brownian

motion [30], PNCs with an extended particle network should exhibit a two-step relaxation with a long tail in the relaxation modulus [31]. Nevertheless, a quantitative prediction is not possible at this moment, due to the lack of information on particle distribution as well as a feasible theoretical model. Fig. 3a shows the evolution of engineering stress in PMMA (dashed line) and PMMA/SiO_2 (red crosses) during and after a step deformation of $\lambda = 1.8$. Due to the presence of nanoparticles, the stress of PMMA/SiO_2 is about 30% higher than that of PMMA. However, contrary to the phenomenology of a two-step relaxation in PNCs with nanoparticle network, there is no sharp drop of stress in PMMA/SiO_2 during the initial phase of relaxation (inset of Fig. 3a) or a slowly decaying tail in the long-time limit. In fact, as shown by the inset of Fig. 3a, the stress relaxation curves of PMMA and PMMA/SiO_2 are parallel to each other. These features indicate an absence of noticeable stress contribution from the nanoparticle-nanoparticle interactions in the PMMA/SiO_2 — a conclusion that is consistent with the SAXS and linear viscoelastic measurements, where no signs of a nanoparticle network are found.

What about the polymer structural anisotropy during stress relaxation? We further performed SANS measurements and analyze the spectra at different elapsed time, $t = 0\tau$, 0.01τ, 0.03τ, 0.1τ, 0.3τ, and 1τ during the stress relaxation, where τ is the terminal relaxation time of the pristine PMMA estimated from the low-frequency crossover of the storage and loss moduli. The inset of Fig. 3b presents the normalized anisotropic coefficients $S_2^0(Q;t)/S_2^0(Q;0)$ of the PNCs (symbols) and the pristine polymer (lines) during the relaxation. Similar to the results of continuous extension, the normalized structural anisotropy of the two samples are almost identical over a length scale from $Q = 0.008$ Å^{-1}=1/(125 Å)$\sim R_g^{-1}$ (inverse of radius of gyration) to $Q = 0.065$ Å^{-1}= 1/(15.4 Å)$\sim l_K^{-1}$ (inverse of Kuhn length) and a time scale up to $\sim \tau$. Furthermore, the previous reported scaling relation for anisotropy relaxation (based on polystyrene and coarse-grain MD simulations) holds true for both the pristine PMMA and PMMA/SiO_2 (Fig. 3b) [25]:

$$\frac{S_2^0(Q;t)}{S_2^0(Q;0)} \approx \exp\left[-(\Gamma t)^{\frac{1}{2}}\right], \tag{3}$$

where the characteristic decay rate $\Gamma \propto QR_g/\tau$. Evidently, the inclusion of NPs does not affect the slow relaxation dynamics of the deformed polymer matrix.

To recap the preceding analysis, our SANS and rheological measurements unambiguously reveal substantial mechanical reinforcement with no enhanced polymer structural anisotropy during both uniaxial extension and subsequent relaxation. The absence of strain amplification in the matrix polymer is especially intriguing, given the prevailing viewpoint that the matrix polymer should undergo larger deformation to fulfill the macroscopic deformation due to the presence of non-deformable inorganic particles [18]. Moreover, the rheological signatures of the relaxation experiments rule out NP-NP interactions as the mechanism for reinforcement. These observations significantly challenge the current molecular understanding of the mechanical reinforcement of PNCs and call for a different explanation of the role of NPs in modifying the deformation of the matrix polymer.

According to the classical hydrodynamic theory for dilute particle suspensions [11, 32–36], the particle distorts the strain field surrounding the nanoparticles, and such an effect propagates far into the bulk, over a distance of a few times of the size of the particle [12]. More importantly, the *net* disturbance of the particle to the strain of the matrix polymer is zero across the matrix. In other words, the hydrodynamic reinforcement theory implies an enhanced mechanical response from the resistance of particles to the straining field with the *average* disturbance of the velocity gradient or deformation gradient field in the bulk being zero [12]. Our experiments, on the other hand, show enhanced stress governed by polymer matrix but no increase of polymer structural anisotropy, in excellent agreement with this picture. Thus, the classical hydrodynamic theory, at the leading order, explains the molecular mechanism of mechanical reinforcement in PNCs — a redistribution of the stress and strain field over a large area surrounding the nanoparticles rather than strain amplification of the entire matrix polymer. The particle-induced redistribution of the stress and strain also leads to an enhancement in the mechanical properties. Nevertheless, a rigorous calculation on the influence of nanoparticles to the stress and strain field in concentrated PNCs is challenging [37], due to the complex geometry and the multi-scale coupling [38, 39] of the polymer-nanoparticle and nanoparticle-nanoparticle interactions, such as the interplay between polymer adsorption, interfacial entanglement, and hydrodynamic force. The detail of strain field distribution requires further investigation.

As far as the scattering problem is concerned, a precise calculation appears to be difficult even for this simple case. However, for a homogeneous system in the small-strain limit, the influence of an elastic deformation on the pair distribution function g(r) can be formally described by a multipole expansion as [40, 41]: $g(\mathbf{r}) - g(r) = \{-[(\mathbf{E}-\mathbf{I})\cdot\mathbf{r}]\cdot\nabla\}g(r) + \frac{1}{2}\{-[(\mathbf{E}-\mathbf{I})\cdot\mathbf{r}]\cdot\nabla\}^2 g(r) + \ldots$, where $\mathbf{E}$ is the deformation gradient tensor and $\mathbf{I}$ is the isotropic tensor. Suppose the particle size is relative large and we are probing the structure at relatively high Q, it can be argued that in this limit the anisotropic pair correlation functions can be averaged in different fluid elements. Truncating the expansion at the first order, it is straightforward to show that the average deformed single-chain structure is indeed not affected by the presence of particles. While our PNC system cannot be regarded as a dilute suspension of silica particles, the results from SANS and rheological experiments suggest that the underlying physical picture is strikingly similar. It is worth noting that the evolutions of both the mechanical signal and structural anisotropy parallel those of the pristine polymer during stress relaxation, which is consistent with the current interpretation. Lastly, we point out that our explanation does not necessarily exclude potentially highly localized response from interfacial polymers in the vicinity of the nanoparticles [42–44].

In summary, the microscopic origin of mechanical reinforcement in deformed polymer nanocomposite melts is investigated through a combination of small-angle neutron scattering and rheology. In contrast to the prevailing viewpoint of the molecular overstraining, strain amplification is not observed by SANS. Similar to the classical picture of Einstein and Smallwood for dilute suspensions, the enhanced mechanical response originates from the resistance of particles to the straining field, whereas the average disturbance of the deformation gradient in the bulk is nearly zero. This finding clarifies a long-standing puzzle regarding the molecular origin of the mechanical reinforcement mechanism in deformed PNCs and provides a new perspective for understanding of the hydrodynamic effect of nanosized particles in viscoelastic medium. While the current experiments focus on the deformation rate in the middle of the rubbery plateau, our conclusions should apply to the entire rubbery regime, where the entanglement dynamics dominates the rheological behavior.

This work was supported, in part, by the Ralph E. Powe Junior Faculty Enhancement Awards from Oak Ridge Associated Universities (ORAU). Y.Y.W. acknowledges support by the U.S. Department of Energy, Office of Science, Office of Basic Energy Sciences, Early Career Research Program Award KC0402010, under contract DE-AC05-00OR22725. Part of this work was conducted at ORNL's Center for Nanophase Materials Sciences, which is a U.S. Department of Energy Office of Science User Facility. The SAXS measurements were performed at Beamline 12-ID-B of Advanced Photon Source, a U.S. Department of Energy (DOE) Office of Science User Facility operated for the DOE Office of Science by Argonne National Laboratory under Contract No. DE-AC02-06CH11357. Access to NGB 30m SANS was provided by the Center for High Resolution Neutron Scattering, a partnership between the National Institute of Standards and Technology and the National Science Foundation under Agreement No. DMR-1508249. Certain commercial equipment, instruments, or materials are identified in this document. Such identification does not imply recommendation or endorsement by the National Institute of Standards and Technology nor does it imply that the products identified are necessarily the best available for the purpose.

[1] J. Jancar, J. F. Douglas, F. W. Starr, S. K. Kumar, P. Cassagnau, A. J. Lesser, S. S. Sternstein, and M. J. Buehler, Current issues in research on structure–property relationships in polymer nanocomposites, Polymer **51**, 3321 (2010).

[2] T. A. Vilgis, G. Heinrich, and M. Klüppel, *Reinforcement of Polymer Nano-Composites: Theory, Experiments and Applications* (Cambridge University Press, 2009).

[3] A. K. Naskar, J. K. Keum, and R. G. Boeman, Polymer matrix nanocomposites for automotive structural components, Nature Nanotechnology **11**, 1026 (2016).

[4] A. C. Balazs, T. Emrick, and T. P. Russell, Nanoparticle polymer composites: where two small worlds meet, Science **314**, 1107 (2006).

[5] Y. Song and Q. Zheng, Concepts and conflicts in nanoparticles reinforcement to polymers beyond hydrodynamics, Pro. Mater. Sci. **84**, 1 (2016).

[6] Y. Song and Q. Zheng, A guide for hydrodynamic reinforcement effect in nanoparticle-filled polymers, Critical Rev. Solid State Mater. Sci. **41**, 318 (2016).

[7] J. Domurath, M. Saphiannikova, and G. Heinrich, The concept of hydrodynamic amplification infilled elastomers, Kautschuk und Gummi Kunststoffe **70**, 40 (2017).

[8] M. M. Rueda, M.-C. Auscher, R. Fulchiron, T. Perie, G. Martin, P. Sonntag, and P. Cassagnau, Rheology and applications of highly filled polymers: A review of current understanding, Prog. Polym. Sci. **66**, 22 (2017).

[9] A. Einstein, Eine neue bestimmung der moleküldimensionen, Ann. Phys. **324**, 289 (1906).

[10] A. Einstein, Berichtigung zu meiner arbeit: Eine neue bestimmung der moleküldimensionen, Ann. Phys. **339**, 591 (1911).

[11] H. M. Smallwood, Limiting law of the reinforcement of rubber, J. Appl. Phys. **15**, 758 (1944).

[12] Supplemental Material.

[13] G. K. Batchelor, The effect of Brownian motion on the bulk stress in a suspension of spherical particles, J. Fluid Mech. **83**, 97 (1977).

[14] L. Mullins and N. R. Tobin, Stress softening in rubber vulcanizates. Part I. use of a strain amplification factor to describe the elastic behavior of filler-reinforced vulcanized rubber, J. Appl. Polym. Sci. **9**, 2993 (1965).

[15] H. S. Varol, F. Meng, B. Hosseinkhani, C. Malm, D. Bonn, M. Bonn, A. Zaccone, and S. H. Parekh, Nanoparticle amount, and not size, determines chain alignment and nonlinear hardening in polymer nanocomposites, Proc. Nat. Acad. Sci. **114**, E3170 (2017).

[16] S. Westermann, M. Kreitschmann, W. Pyckhout-Hintzen, D. Richter, E. Straube, B. Farago, and G. Goerigk, Matrix chain deformation in reinforced networks: a SANS approach, Macromolecules **32**, 5793 (1999).

[17] R. Pérez-Aparicio, M. Schiewek, J. L. Valentín, H. Schneider, D. R. Long, M. Saphiannikova, P. Sotta, K. Saalwächter, and M. Ott, Local chain deformation and overstrain in reinforced elastomers: An NMR study, Macromolecules **46**, 5549 (2013).

[18] J. Wang, Y. Guo, W. Yu, C. Zhou, and P. Steeman, Linear and nonlinear viscoelasticity of polymer/silica nanocomposites: an understanding from modulus decomposition, Rheol. Acta **55**, 37 (2016).

[19] A. Botti, W. Pyckhout-Hintzen, D. Richter, V. Urban, and E. Straube, A microscopic look at the reinforcement of silica-filled rubbers, J. Chem. Phys. **124**, 174908 (2006).

[20] N. Jouault, F. Dalmas, S. Said, E. Di Cola, R. Schweins, J. Jestin, and F. Boué, Direct small-angle-neutron-scattering observation of stretched chain conformation in nanocomposites: More insight on polymer contributions in mechanical reinforcement, Phys. Rev. E **82**, 031801 (2010).

[21] N. Jouault, F. Dalmas, S. Said, E. Di Cola, R. Schweins, J. Jestin, and F. Boué, Direct measurement of polymer chain conformation in well-controlled model nanocomposites by combining sans and saxs, Macromolecules **43**, 9881 (2010).

[22] A. Botti, W. Pyckhout-Hintzen, D. Richter, V. Urban, E. Straube, and J. Kohlbrecher, Silica filled elastomers: polymer chain and filler characterization in the undeformed state by a SANS–SAXS approach, Polymer **44**, 7505 (2003).

[23] A. Genix and J. Oberdisse, Structure and dynamics of polymer nanocomposites studied by x-ray and neutron scattering techniques, Curr. Opin. Colloid & Interface Sci. **20**, 293 (2015).

[24] Y. Wang, W. Wang, K. Hong, C. Do, and W.-R. Chen, Quanti-

tative examination of a fundamental assumption in small-angle neutron scattering studies of deformed polymer melts, Polymer **204**, 122698 (2020).

[25] C. N. Lam, W.-S. Xu, W.-R. Chen, Z. Wang, C. B. Stanley, J.-M. Y. Carrillo, D. Uhrig, W. Wang, K. Hong, Y. Liu, L. Porcar, C. Do, G. S. Smith, B. G. Sumpter, and Y. Wang, Scaling behavior of anisotropy relaxation in deformed polymers, Phys. Rev. Lett. **121**, 117801 (2018).

[26] Z. Wang, C. N. Lam, W.-R. Chen, W. Wang, J. Liu, Y. Liu, L. Porcar, C. B. Stanley, Z. Zhao, K. Hong, and Y. Wang, Fingerprinting molecular relaxation in deformed polymers, Phys. Rev. X **7**, 031003 (2017).

[27] J. Yang, M. Melton, R. Sun, W. Yang, and S. Cheng, Decoupling the polymer dynamics and the nanoparticle network dynamics of polymer nanocomposites through dielectric spectroscopy and rheology, Macromolecules **53**, 302 (2020).

[28] N. Jouault, M. K. Crawford, C. Chi, R. J. Smalley, B. Wood, J. Jestin, Y. B. Melnichenko, L. He, W. E. Guise, and S. K. Kumar, Polymer chain behavior in polymer nanocomposites with attractive interactions, ACS Macro Lett. **5**, 523 (2016).

[29] J. S. Higgins and H. C. Benoît, *Polymers and Neutron Scattering* (Clarendon Press, Oxford, 1994).

[30] P. J. Griffin, V. Bocharova, L. R. Middleton, R. J. Composto, N. Clarke, K. S. Schweizer, and K. I. Winey, Influence of the bound polymer layer on nanoparticle diffusion in polymer melts, ACS Macro Lett. **5**, 1141 (2016).

[31] Z. Zhu, T. Thompson, S.-Q. Wang, E. D. von Meerwall, and A. Halasa, Investigating linear and nonlinear viscoelastic behavior using model silica-particle-filled polybutadiene, Macromolecules **38**, 8816 (2005).

[32] H. Hasimoto, A sphere theorem on the stokes equation for axisymmetric viscous flow, J. Phys. Soc. Jpn. **11**, 793 (1956).

[33] G. K. Batchelor, The stress system in a suspension of force-free particles, J. Fluid Mech. **41**, 545 (1970).

[34] A. T. Chwang and T. Wu, Hydromechanics of low-Reynolds-number flow. Part 2. Singularity method for Stokes flows, J. Fluid Mech. **67**, 787 (1975).

[35] D. J. Jeffrey and A. Acrivos, The rheological properties of suspensions of rigid particles, AIChE J. **22**, 417 (1976).

[36] E. Guazzelli and J. F. Morris, *A Physical Introduction to Suspension Dynamics* (Cambridge University Press, 2011).

[37] J. Mewis and N. J. Wagner, *Colloidal Suspension Rheology* (Cambridge University Press, 2012).

[38] Q. Zeng, A. Yu, and G. Lu, Multiscale modeling and simulation of polymer nanocomposites, Prog. Polym. Sci. **33**, 191 (2008).

[39] G. G. Vogiatzis and D. N. Theodorou, Structure of polymer layers grafted to nanoparticles in silica — polystyrene nanocomposites, Macromolecules **46**, 4670 (2013).

[40] J. H. Irving and J. G. Kirkwood, The statistical mechanical theory of transport processes. IV The equations of hydrodynamics, J. Chem. Phys. **18**, 817 (1950).

[41] G.-R. Huang, B. Wu, Y. Wang, and W.-R. Chen, Characterization of microscopic deformation through two-point spatial correlation functions, Phys. Rev. E **97**, 012605 (2018).

[42] S. Cheng, V. Bocharova, A. Belianinov, S. Xiong, A. Kisliuk, S. Somnath, A. P. Holt, O. Ovchinnikova, S. Jesse, H. Martin, T. Etampawala, M. Dadmun, and A. P. Sokolov, Unraveling the mechanism of nanoscale mechanical reinforcement in glassy polymer nanocomposites, Nano letters **16**, 3630 (2016).

[43] S. Cheng, B. Carroll, W. Lu, F. Fan, J.-M. Y. Carrillo, H. Martin, A. P. Holt, N.-G. Kang, V. Bocharova, J. W. Mays, B. G. Sumpter, M. Dadmun, and A. P. Sokolov, Interfacial properties of polymer nanocomposites: Role of chain rigidity and dynamic heterogeneity length scale, Macromolecules **50**, 2397 (2017).

[44] B. D. Vogt, Mechanical and viscoelastic properties of confined amorphous polymers, J. Polym. Sci. Part B: Polym. Phys. **56**, 9 (2018).